

Suppression of Type I IFN Signaling in Tumors Mediates Resistance to Anti-PD-1 Treatment That Can Be Overcome by Radiotherapy

Xiaohong Wang¹, Jonathan E. Schoenhals¹, Ailin Li¹, David R. Valdecanas¹, Huiping Ye², Fenglin Zang³, Chad Tang⁴, Ming Tang⁵, Chang-Gong Liu⁶, Xiuping Liu⁶, Sunil Krishnan⁴, James P. Allison⁷, Padmanee Sharma⁸, Patrick Hwu⁹, Ritsuko Komaki⁴, Willem W. Overwijk¹⁰, Daniel R. Gomez⁴, Joe Y. Chang⁴, Stephen M. Hahn⁴, Maria Angelica Cortez¹, and James W. Welsh⁴

Abstract

Immune checkpoint therapies exhibit impressive efficacy in some patients with melanoma or lung cancer, but the lack of response in most cases presses the question of how general efficacy can be improved. In addressing this question, we generated a preclinical tumor model to study anti-PD-1 resistance by *in vivo* passaging of Kras-mutated, p53-deficient murine lung cancer cells ($p53^{R172H\Delta g/+}K-ras^{LA1/+}$) in a syngeneic host exposed to repetitive dosing with anti-mouse PD-1 antibodies. PD-L1 (CD274) expression did not differ between the resistant and parental tumor cells. However, the expression of important molecules in the antigen presentation pathway, including MHC class I and II, as well as β 2-microglobulin, were significantly downregulated in the anti-PD-1-resistant

tumors compared with parental tumors. Resistant tumors also contained fewer CD8⁺ (CD8 α) and CD4⁺ tumor-infiltrating lymphocytes and reduced production of IFN γ . Localized radiotherapy induced IFN β production, thereby elevating MHC class I expression on both parental and resistant tumor cells and restoring the responsiveness of resistant tumors to anti-PD-1 therapy. Conversely, blockade of type I IFN signaling abolished the effect of radiosensitization in this setting. Collectively, these results identify a mechanism of PD-1 resistance and demonstrate that adjuvant radiotherapy can overcome resistance. These findings have immediate clinical implications for extending the efficacy of anti-PD-1 immune checkpoint therapy in patients. *Cancer Res*; 77(4); 839–50. ©2016 AACR.

Introduction

The interaction between programmed cell death receptor-1 (PD-1) and its ligand (PD-L1) inhibits T-cell proliferation, survival, and effector functions, which limit antigen-specific T-cell responses and antitumor immunity (1). Antibodies

blocking PD-1/PD-L1 have led to impressive durable clinical responses in some patients with melanoma, lung cancer, or renal cell carcinoma; anti-PD-1/PD-L1 therapies, given as single-agent therapy, have produced objective response rates ranging from 15% to 25% in patients with chemotherapy-refractory non-small cell lung carcinoma (NSCLC; refs. 2–4) and 33% in advanced squamous cell lung cancer (SCLC; ref. 3). Nevertheless, large proportions of patients do not respond to anti-PD-1/PD-L1 immunotherapies. Some clinical studies have suggested that PD-L1 expression on tumor tissues correlates with objective response to the anti-PD-1 therapy (5–7), but response rates among patients with PD-L1-positive tumors are less than 50% in most studies (6, 7), and some patients with tumors that express little or no PD-L1 still show some response to anti-PD-1/anti-PD-L1 therapy (6, 7). This suggests that PD-L1 expression is not the sole mechanism that determines whether tumors respond to anti-PD-1/PD-L1 treatment. This observation raises fundamental questions about additional mechanisms underlying nonresponse and potential strategies to overcome anti-PD-1/PD-L1 resistance. We report here our generation of an anti-PD-1-resistant lung cancer mouse model in which PD-L1 expression was not changed on the anti-PD-1-resistant tumors. The anti-PD-1-resistant tumors showed downregulation of MHC class I and II proteins, as well as β 2-microglobulin (β 2M) and reduced infiltration and activation of CD4⁺ and CD8⁺ T cells compared with parental tumors. We further found that delivery of localized radiation induced type I IFN production, upregulated MHC class I expression, and restored

¹Department of Experimental Radiation Oncology, The University of Texas MD Anderson Cancer Center, Houston, Texas. ²Department of Otolaryngology Head and Neck Surgery, The Affiliated Baiyun Hospital of Guiyang Medical University, Guiyang Medical University, Guiyang, China. ³Department of Pathology, The University of Texas MD Anderson Cancer Center, Houston, Texas. ⁴Department of Radiation Oncology, The University of Texas MD Anderson Cancer Center, Houston, Texas. ⁵Genomic Medicine, The University of Texas MD Anderson Cancer Center, Houston, Texas. ⁶Experimental Therapeutics, The University of Texas MD Anderson Cancer Center, Houston, Texas. ⁷Department of Immunology, The University of Texas MD Anderson Cancer Center, Houston, Texas. ⁸Department of Genitourinary Medical Oncology, The University of Texas MD Anderson Cancer Center, Houston, Texas. ⁹Department of Cancer Medicine, The University of Texas MD Anderson Cancer Center, Houston, Texas. ¹⁰Department of Melanoma Medical Oncology, The University of Texas MD Anderson Cancer Center, Houston, Texas.

Note: Supplementary data for this article are available at Cancer Research Online (<http://cancerres.aacrjournals.org/>).

Corresponding Author: James W. Welsh, Department of Radiation Oncology, The University of Texas MD Anderson Cancer Center, 1515 Holcombe Blvd, Unit 0097, Houston, TX 77005. Phone: 713-563-2447; Fax: 713-563-2366; E-mail: jwelsh@mdanderson.org

doi: 10.1158/0008-5472.CAN-15-3142

©2016 American Association for Cancer Research.

response to anti-PD-1 in our anti-PD-1-resistant model; blockade of type I IFN signaling via anti-IFN α/β receptor (IFNAR) antibodies abolished the effect of radiation on reestablishing the response to anti-PD-1. Ultimately, our studies reveal an important mechanism of anti-PD-1 resistance and suggest that radiation may constitute a therapeutic strategy for overcoming resistance to anti-PD-1 therapy.

Materials and Methods

Cell lines and drugs

The 344SQ parental cell line (344SQ_P) is a metastatic mouse lung cancer cell line derived from a spontaneous subcutaneous metastatic lesion in $p53^{R172H\Delta g/+}K-ras^{LA1/+}$ mice (8, 9). This cell line was a generous gift from Dr. Jonathan Kurie (MD Anderson Cancer Center, Houston, TX). Murine anti-mouse PD-1 (DX-400) antibodies from Merck were diluted to 2 mg/mL in 20 mmol/L sodium acetate and 7% sucrose, pH 5.5, according to Merck's instructions. Mouse IgG1 isotype control antibody (also from Merck) was diluted to 2 mg/mL in 75 mmol/L NaCl, 10 mmol/L phosphate, and 3% sucrose, pH 7.3, according to Merck's instructions. Both antibodies were fully murinized. An anti-PD-1-resistant cell line (344SQ_R), derived as described below, and 344SQ_P were then used for *in vivo* studies. Both cell lines were validated by DDC Medical (<http://ddcmedical.com>) by short tandem repeat (STR) DNA fingerprinting. All animal procedures were reviewed and approved by The University of Texas MD Anderson Cancer Center Animal Care and Use Committee.

Tumor challenge and treatments

The anti-PD-1 cell line was generated as follows: The 344SQ parental cancer cells (0.5×10^6 in 50 μ L of sterile PBS) were injected subcutaneously into the leg of syngeneic 129Sv/ev mice (female, 12–16 weeks old). The mice were then given intraperitoneal injections of anti-PD-1 or control IgG antibodies (10 mg/kg), starting on day 4 after tumor cell inoculation and continuing twice per week for a total of 4 or 5 doses. A nonresponsive tumor was isolated from an unirradiated tumor in mice bearing two tumors treated with anti-PD-1 and radiation. The nonresponsive tumor was digested into single cells and cultured *in vitro* for about 2 to 3 weeks, and subjected to 4 cycles of sequential *in vivo* passage in the syngeneic mice, with anti-PD-1 treatment continuing throughout (Fig. 1A). Those cells, having shown resistance to anti-PD-1 treatment *in vivo*, were named the anti-PD-1-resistant 344SQ (344SQ_R) cell line. Both parental and resistant cell lines were authenticated by STR DNA fingerprinting by DDC Medical.

The growth rate of the tumor mass was recorded as measurements of tumor length (L) and width (W) with calipers. Tumor volume (V) was calculated as $V = W^2 \times L/2$. For the combined radiation plus anti-PD-1 therapy studies, tumor-bearing mice were irradiated when the average tumor volume was 100 mm³ (typically 10–14 days after inoculation of 344SQ_P cells or 7–9 days after inoculation of 344SQ_R cells); the first dose of anti-PD-1 (10 mg/kg) was given on the same day as the first fraction of radiation and continued for additional 3 to 4 doses. For experiments involving blockade of type I IFN signaling, anti-mouse IFNAR-1 antibody (BioLegend, 1 mg/kg) was injected intratumorally once a day for 14 days, starting on the

day of the first dose of anti-PD-1. In some studies, lungs were collected at the end of the experiment and fixed in Bouin's solution (Sigma) for 3 days, after which lung metastatic nodules were counted. For experiments to investigate intratumoral lymphocyte populations, 1×10^6 cancer cells in 50 μ L of PBS were subcutaneously injected into the right leg of 129Sv/ev mice, and tumors were harvested and analyzed 7 days after anti-PD-1 treatment. Radiation involved restraining the mice in a jig, after which the primary tumors in the right leg were irradiated (while the remainder of the mouse was shielded) with a self-shielding Cs-137 Suitatron model IR-64 irradiator. A total dose of 36 Gy was delivered in 3 fractions over 3 days.

Protein extraction and Western blot analysis

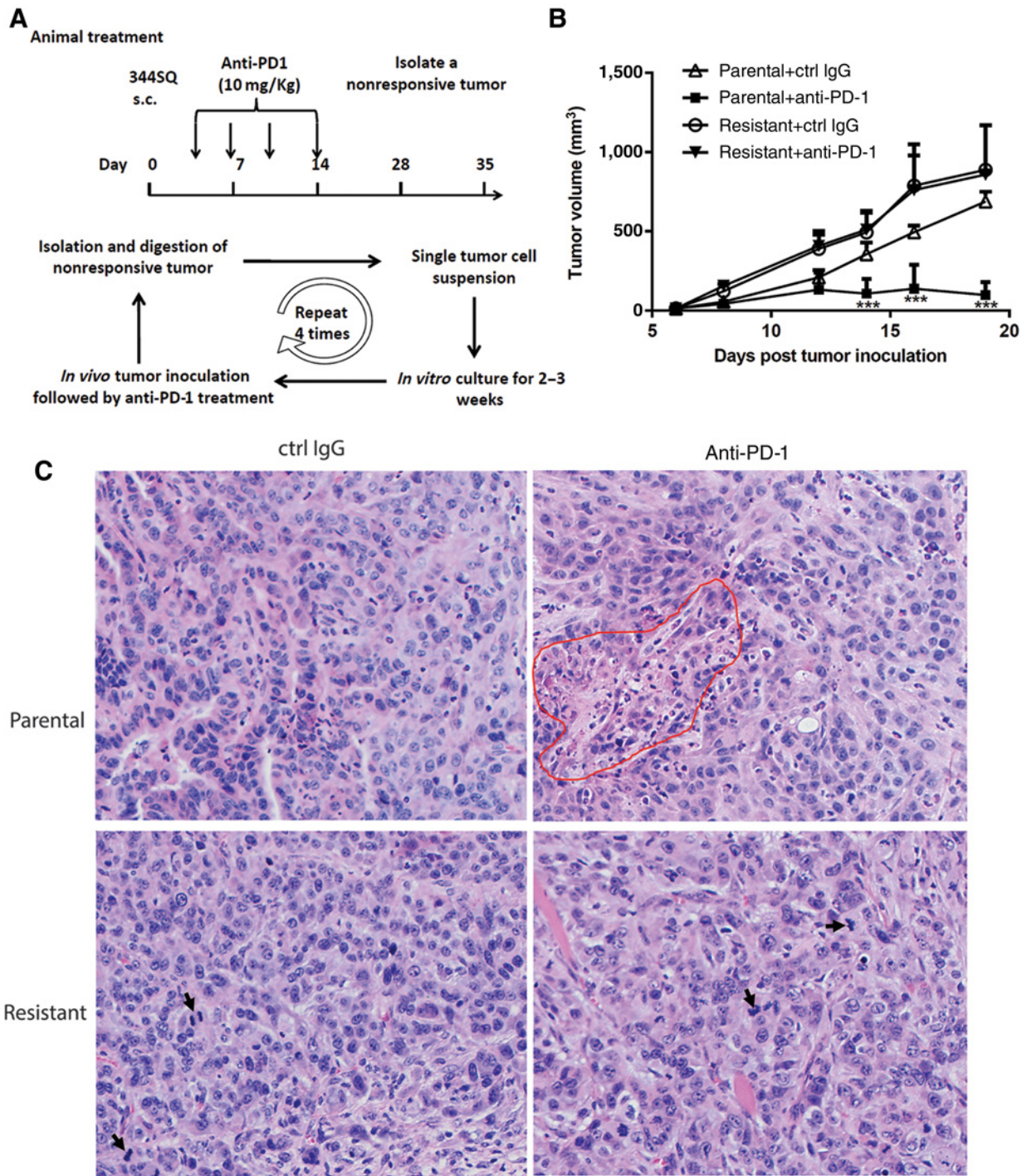
Total protein was extracted by using NP40 lysis buffer (0.5% NP40, 250 mmol/L NaCl, 50 mmol/L HEPES, 5 mmol/L ethylenediaminetetraacetic acid, and 0.5 mmol/L egtazic acid) supplemented with protease inhibitors cocktails (Sigma-Aldrich). Lysates were centrifuged at $10,000 \times g$ for 10 minutes, and the supernatant was collected for experiments. Protein lysates (40 μ g) were resolved on denaturing gels with 4% to 20% SDS-PAGE and transferred to nitrocellulose membranes (Bio-Rad Laboratories). Membranes were probed with the following antibodies: primary antibodies, anti- β 2M (Santa Cruz Biotechnology), anti-vinculin (Cell Signaling Technology), and secondary antibody labeled by horseradish peroxidase (Amersham GE Healthcare). The secondary antibody was visualized by using a chemiluminescent reagent Pierce ECL Kit (Thermo Fisher Scientific).

Tumor-infiltrating immune cell isolation

Mice used for functional experiments were killed on day 7 after anti-PD-1 treatment. Tumors, spleen, and blood were collected. Tumor tissues were minced into small pieces and digested in 250 μ g/mL Liberase TR (Roche) and 20 μ g/mL DNase I (Roche) at 37°C for 30 minutes, filtered, and washed with PBS + 1 μ mol/L ethylenediaminetetraacetic acid. The cell suspensions were layered over Histopaque-1077 (Sigma-Aldrich) at 1:1 v/v and centrifuged at $400 \times g$ for 30 minutes. The tumor-infiltrating immune cells in the interphase were collected and washed with PBS + 2% FBS, followed by staining with various markers as described below.

Cell staining, flow cytometry, and quantification

Tumor cells or tumor-associated immune cells were blocked with anti-mouse CD16/32 antibody (FcR blocker) for 10 minutes at room temperature and then stained with anti-CD45-pacific blue (30-F11), anti-CD4-FITC (GK1.5), anti-CD8-PerCP-Cy5.5 (53-6.7), anti-CD11c -PE (N418), anti-F4/80-PerCP/Cy5.5 (BM8), anti-CD11b-APC/Cy7 (M1/70), anti-Gr-1-PE/Cy7 (RB6-8C5), anti-PD-L1-APC (10F.9G2), PD-1-PE/Cy7 (RMP1-30), I-A/I-E-PE/Cy5 (M5/114.15.2), H-2K^b-PE (AF6-88.5), and/or H-2D^p-FITC (KH95) at room temperature for 30 minutes. All antibodies were purchased from BioLegend. For intracellular staining of IFN γ , cells were fixed and permeabilized according to the manufacturer's instructions (BioLegend) and stained with anti-IFN γ -APC (XMG1.2). All samples were acquired with LSRII flow cytometer and analyzed with FlowJo software (version 10.0.7). Absolute numbers of T cells per mg of tumor were calculated as follows: numbers of an

**Figure 1.**

Generation of an anti-PD-1-resistant lung tumor mouse model. **A**, Schematic illustration. 344SQ mouse lung cancer cells were subcutaneously injected into the flank the syngeneic 129Sv/ev mice on day 0. Anti-mouse PD-1 or isotype control (ctrl) IgG antibodies (10 mg/kg) were administered intraperitoneally on days 3, 7, 10, and 14. Tumor growth was monitored for up to 4 weeks. A nonresponsive tumor was isolated and digested into a single-cell suspension. Tumor cells were cultured *in vitro* for 2 to 3 weeks and then reinoculated into 129Sv/ev mice, followed by anti-PD-1 treatment. This procedure was repeated for four cycles. **B**, Representative tumor growth curve of parental 344SQ cells and the anti-PD-1-resistant 344SQ cells upon control IgG or anti-PD-1 treatment. Data represented as mean \pm SD from an n of 5. ***, $P < 0.001$, multiple t tests; experiments were also repeated at least three times. **C**, Representative picture of hematoxylin and eosin staining of parental and anti-PD-1-resistant tumors (magnification, $\times 200$). Red enclosed area, tumor necrosis; black arrows, mitotic tumor cells.

Table 1. Morphologic features of parental and resistant tumors

Morphologic features	Tumor cell type and treatment condition			
	Parental + Control IgG	Parental + Anti-PD-1	Resistant + Control IgG	Resistant + Anti-PD-1
Tubular formation ^a	Yes	Yes	None or little	None or little
Necrosis rate mean (%±SD) ^a	7.3 ± 2.9	22.8 ± 18 ^b	9 ± 4.8	10.9 ± 13.7
Cell size ^c	>4 RBC	>4 RBC	>4 RBC	>4 RBC
Nuclear/cytoplasm ratio ^c	50–80	50–80	>80	>80
Nuclear pleomorphism ^a	Mild	Mild	Marked	Marked
Mitotic count median per field ^c (25%–75%)	8 (5–10)	9 (5–10)	31 (30–50)	37 (30–50)
Immune cell infiltration ^a	Moderate	High	Discrete	Discrete

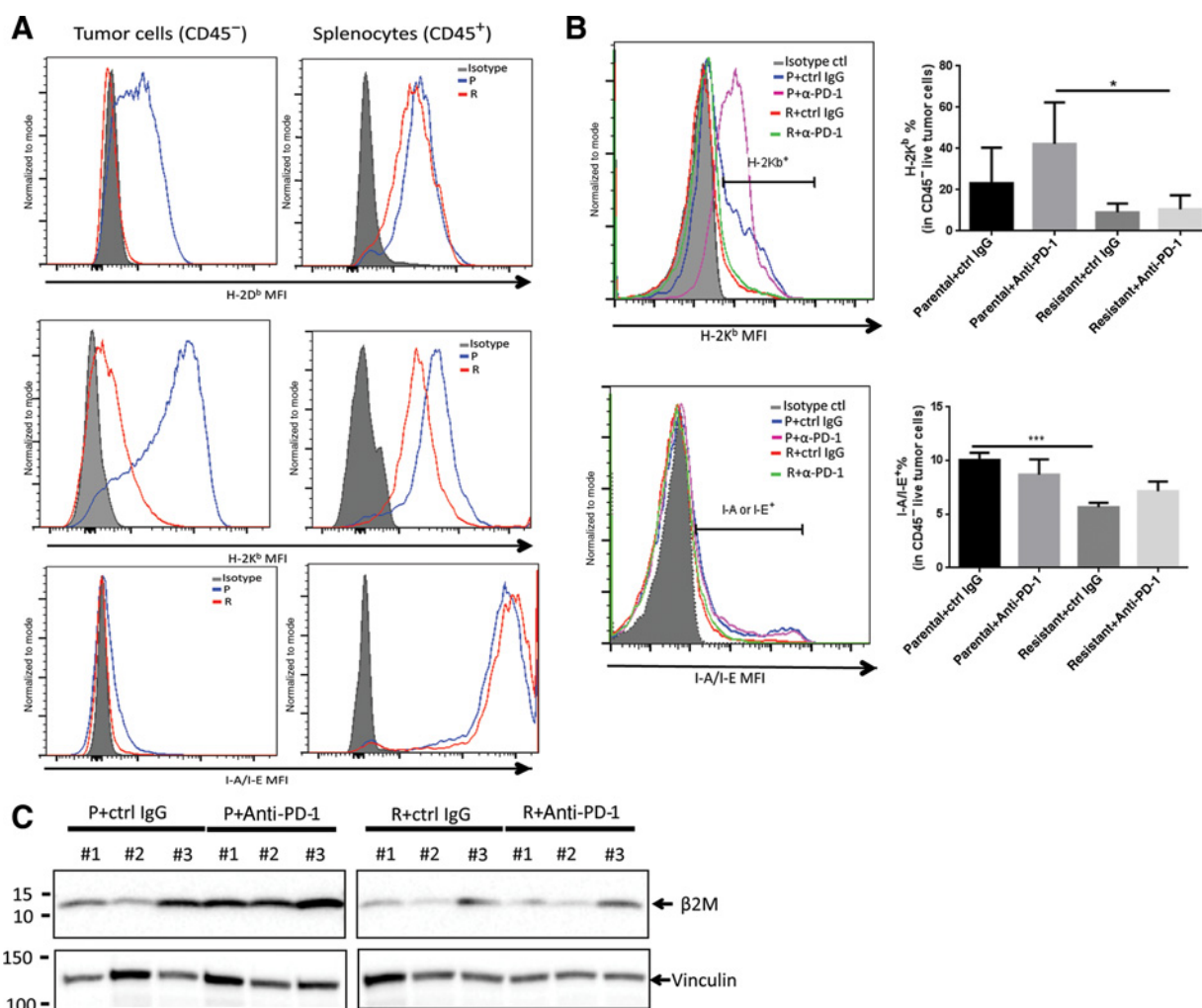
Abbreviation: RBC, red blood cell.

^aFeatures are evaluated in ×200 magnifications.^b*P* < 0.05 versus parental plus control IgG group.^cFeatures are evaluated in ×400 magnifications.

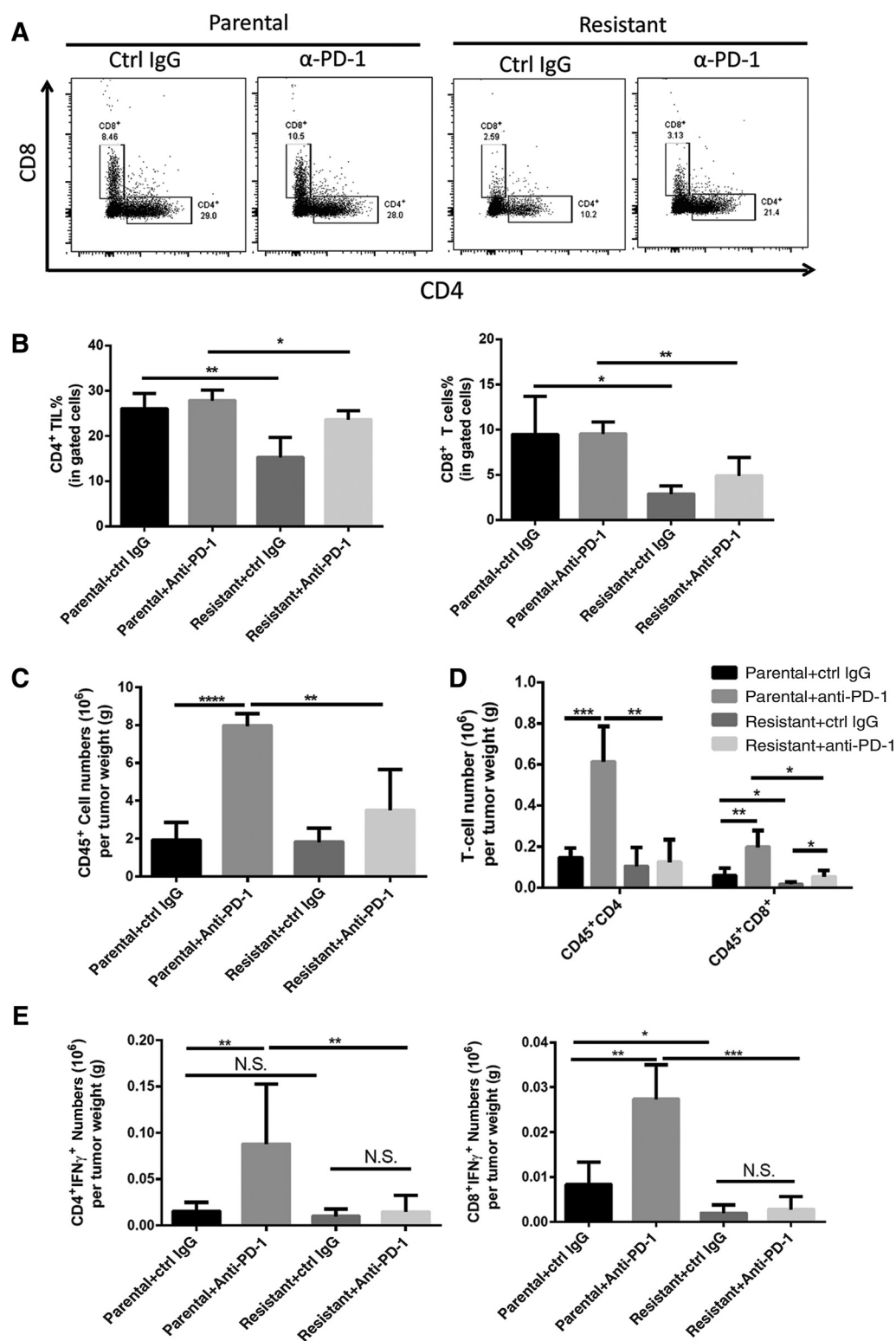
individual immune cell subset = (numbers of isolated tumor-associated immune cell counts × CD45⁺% × the individual immune cell subset %)/tumor weight.

Flow cytometry–based Multiplex for cytokine analysis

Multi-Analyte Flow Assay Kits for IFN γ , IFN β , and TNF α were purchased from BioLegend (LEGENDplex). Plasma samples

**Figure 2.**

Downregulation of MHC molecule expression on anti-PD-1-resistant tumors. **A**, Flow cytometry studies of MHC class I (H-2D^b and H-2K^b) and MHC class II (I-A/I-E) expression on 344SQ_P and 344SQ_R tumor cells (gated on CD45⁻) after cocultured with syngeneic splenocytes (gated on CD45⁺). MFI, mean fluorescence intensity. **B**, H-2K^b and I-A/I-E expression on the parental and anti-PD-1-resistant tumors isolated from tumor-bearing mice with anti-PD-1 or control (ctrl) IgG treatment. **C**, Western blotting of β2M in parental and resistant tumor tissues. Vinculin was used as a loading control. *, *P* < 0.05; ***, *P* < 0.001 in Student *t* tests; data represent means ± SD for an *n* of 5, with experiments repeated at least three times.

**Figure 3.**

Reduced infiltration and function of TILs in anti-PD-1-resistant tumors. **A**, Representative flow cytometry staining of CD4⁺ and CD8⁺ T cells in immune cells isolated from parental and anti-PD-1-resistant tumors. Ctrl, control. **B**, Percentages of CD45⁺CD4⁺ and CD45⁺CD8⁺ T cells in the gated lymphocytes isolated from tumors. **C** and **D**, Total numbers of tumor-infiltrating immune cells (CD45⁺; **C**) and CD45⁺CD4⁺ and CD45⁺CD8⁺ T cells (**D**) isolated from parental and anti-PD-1-resistant tumors. **E**, Total numbers of IFN_γ-producing CD4⁺ and CD8⁺ TILs in tumors. Data represent means ± SD for an *n* of 5, with experiments repeated at least three times. *, *P* < 0.05; **, *P* < 0.01 in Student *t* tests; N.S., not statistically significant.

Wang et al.

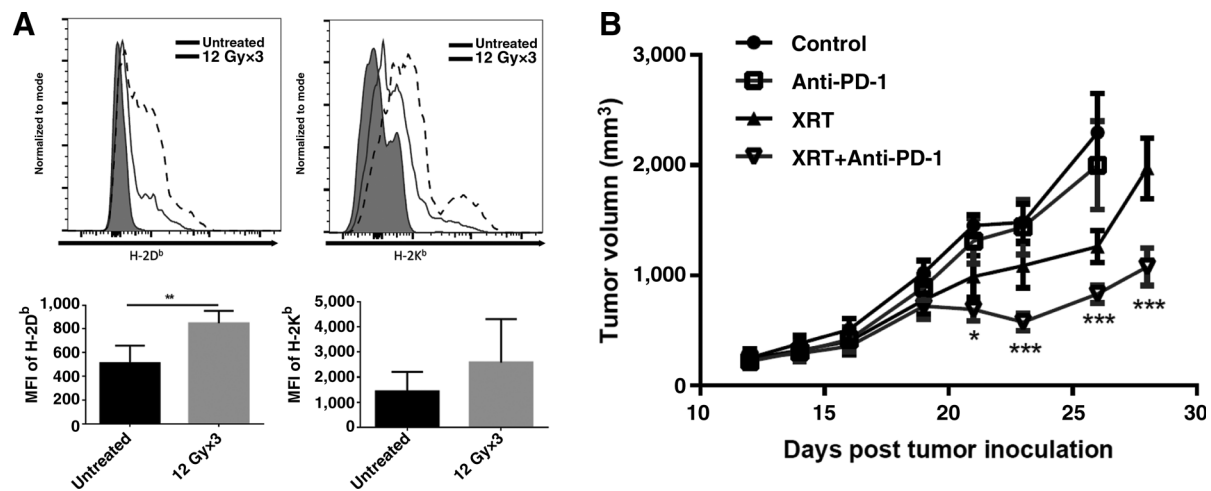


Figure 4.

Radiation increases MHC class I expression and overcomes anti-PD-1 resistance. Mice bearing anti-PD-1-resistant 344SQ tumors were either untreated or irradiated with three 12-Gy fractions. At 5 days after radiation, tumors were isolated, digested into single cells, and stained with live/dead dye, fluorochrome-conjugated CD45, and H-2D^b and H-2K^b antibodies. Tumor cells were gated on a CD45⁺ population. **A**, Radiation significantly increased MHC class I (H-2D^b) expression on the anti-PD-1-resistant tumors. MFI, mean fluorescence intensity. **B**, Radiation resensitized tumors, which allowed the tumors to respond to anti-PD-1 treatment. 344SQ_R cells were inoculated into syngeneic 129Sv/ev mice. At 8 days after inoculation, tumors had reached about 100 mm³ and were irradiated with three 12-Gy fractions over 3 days. The first dose of anti-PD-1 (10 mg/kg) was given on the same day as the first radiation dose and continued for three more doses (twice per week). $P < 0.001$ for XRT versus control groups at days 19, 21, 23, and 26; *, $P < 0.05$; **, $P < 0.01$; ***, $P < 0.001$ for XRT + anti-PD-1 versus XRT groups at days 21, 23, 26, and 28. Data represent means \pm SD for an n of 7 to 8 per group, with experiments repeated three times.

collected from mice were diluted 2-fold with assay buffer according to the manufacturer's instructions. A 96-well v-bottom microplate was pre-wet with 100 μ L wash buffer. Standards were serially diluted according to the manufacturer's instructions. Standards or samples were added in duplicate to the plate, followed by adding antibody-immobilized beads and incubating at room temperature for 2 hours. After incubation with streptavidin-conjugated phycoerythrin for 30 minutes, the samples were washed once, resuspended in wash buffer, and read on a flow cytometer (BD LSR II). After data acquisition, the flow cytometry standard files were analyzed by using BioLegend's LEGENDplex data analysis software to calculate the concentrations of individual cytokines.

Hematoxylin and eosin staining and histopathology evaluation

For these analyses, tumor tissues were removed, fixed in 10% buffered formalin, embedded in paraffin, and stained with hematoxylin and eosin by the Research Histological Core Facility at MD Anderson Cancer Center (Houston, TX). Images of tumor tissue sections at $\times 200$ and $\times 400$ magnifications were acquired with an Olympus BX41 microscope and scored by a pathologist according to histopathologic grading as described previously (10, 11).

Statistical analyses

Data were analyzed with Prism 6.0 (GraphPad Software). Experiments were repeated two to four times. Unpaired Student t tests were used to analyze most data; the exception was tumor growth curves, which were analyzed with multiple t tests for each time points. All reported P values are two-sided and were considered significant at the level of 5%.

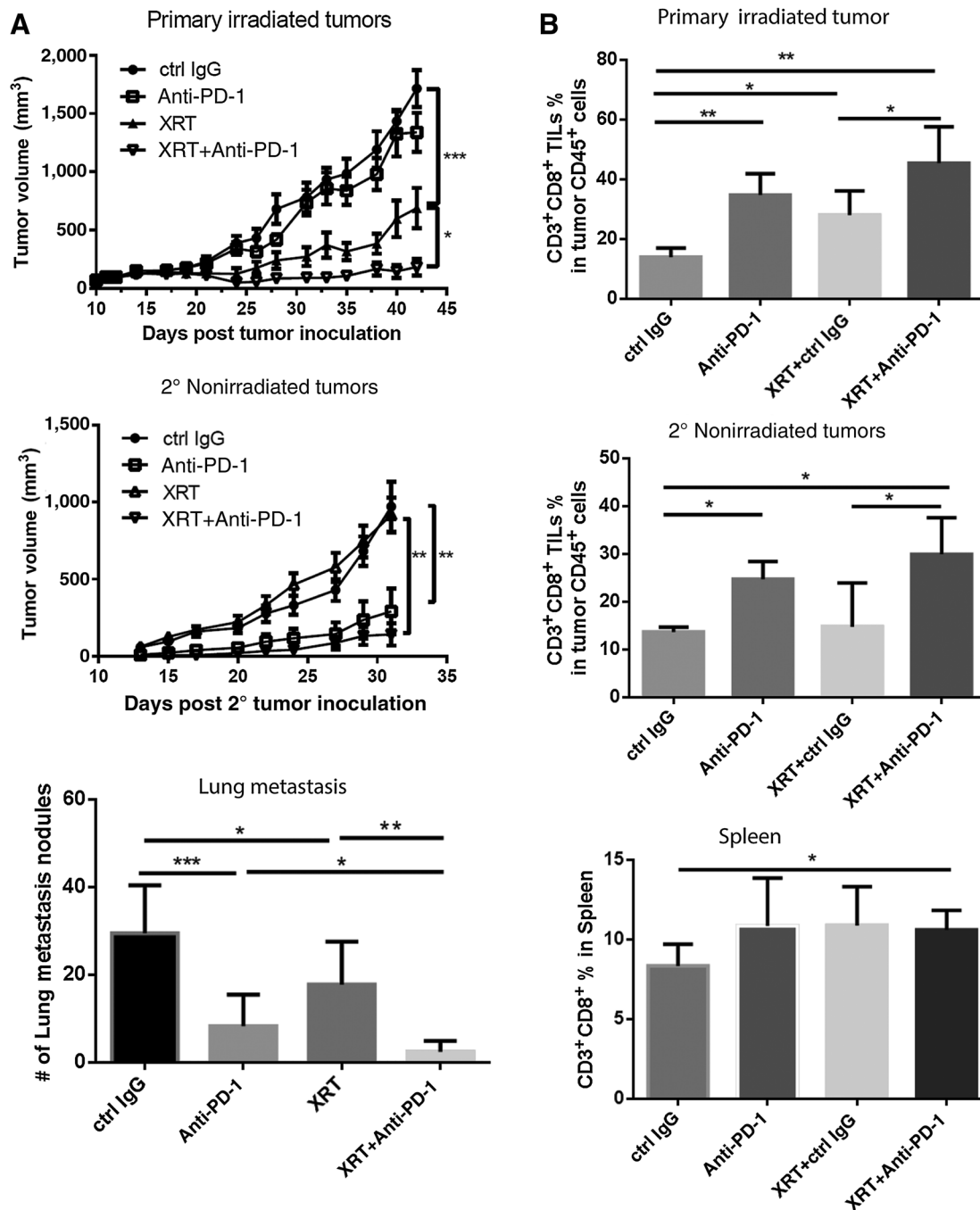
Results

Confirming lung cancer cell sensitivity and resistance to anti-PD-1 *in vivo*

Mice were inoculated with 344SQ_P cells or 344SQ_R cells (derived as shown in Fig. 1A). Tumors formed by the 344SQ_P cells shrank significantly after the mice had been treated with anti-PD-1, but anti-PD-1 had no effect on the *in vivo* tumor growth of 344SQ_R cells when treatment started on day 4 after tumor cell inoculation (Fig. 1B). The 344SQ_R tumors also grew much faster than did the parental tumors *in vivo*. Histopathologic analysis showed that 344SQ_P tumors retained some degree of tubular formation, a feature of differentiated adenocarcinomas morphology, whereas 344SQ_R tumors were more diffuse and poorly differentiated (Fig. 1C; Table 1). Furthermore, 344SQ_R tumors had significantly increased mitosis, more nuclear pleomorphism, and less immune cell infiltration than did the 344SQ_P tumors (Fig. 1C; Table 1). Anti-PD-1 treatment led to increased necrosis in the 344SQ_P tumors but not in 344SQ_R tumors (Fig. 1C; Table 1). Notably, the 344SQ_R tumors, which grew faster with more dividing cells, had higher basal necrosis levels than did 344SQ_P tumors (Table 1), perhaps because fast-growing tumors tend to have higher levels of tumor necrosis (12).

No difference in PD-L1 expression on the parental and anti-PD-1-resistant tumors

Because clinical studies have suggested that PD-L1 expression on tumor tissues correlates with objective response to anti-PD-1 therapy (5–7), we next studied the expression of PD-L1 on the parental and resistant tumor cells. The cell lines from *in vitro* culture showed similar PD-L1 expression levels

**Figure 5.**

Radiation plus anti-PD-1 induces tumor regression and increases proportions of CD8⁺ T cells in both irradiated and nonirradiated tumors. **A**, Radiation plus anti-PD-1 synergistically enhanced the antitumor response by controlling both irradiated tumors and other, nonirradiated, tumors and by reducing the number of spontaneous lung metastases in the 344SQ parental tumor model. 2°, secondary. Primary tumors were established in the right leg by subcutaneous injection of 1×10^6 344SQ_P cells into 129Sv/ev mice. Other nonirradiated tumors were established on the left leg by subcutaneous inoculation of the same amount of 344SQ_P cells in the same mouse on day 10 after primary tumor inoculation. On day 14, when the primary tumors had reached about 100 mm³, primary tumors were irradiated with three 12-Gy fractions over 3 days. Anti-PD-1 treatment was given as described for Fig. 4B; $n = 7$ to 8 per group. In the primary irradiated tumors, $P < 0.01$ for XRT + anti-PD-1 versus anti-PD-1 groups from day 21 to 42 (the endpoint), and $P < 0.05$ or < 0.01 for XRT + anti-PD-1 versus XRT groups from day 33 to 42. In the nonirradiated tumors, P values were < 0.05 or < 0.01 for control (ctrl) versus anti-PD-1 groups from day 13 to 31 (the endpoint), and P values were < 0.01 or < 0.001 for XRT versus XRT + anti-PD-1 groups from day 13 until the end of the experiment. **B**, Radiation plus anti-PD-1 treatment increased the proportion of CD8⁺ T cells in both irradiated and nonirradiated tumors. For these experiments, 344SQ_P cancer cells (1×10^6) were injected in the right leg and 2×10^5 cells in the left leg of mice on the same day. Radiation and anti-PD-1 treatments were the same as described for **A**. Tumors and spleen were collected on day 7 after radiation treatment. $n = 5$ per group. Data represent means \pm SD, with experiments repeated three times. *, $P < 0.05$; **, $P < 0.01$; ***, $P < 0.001$.

Wang et al.

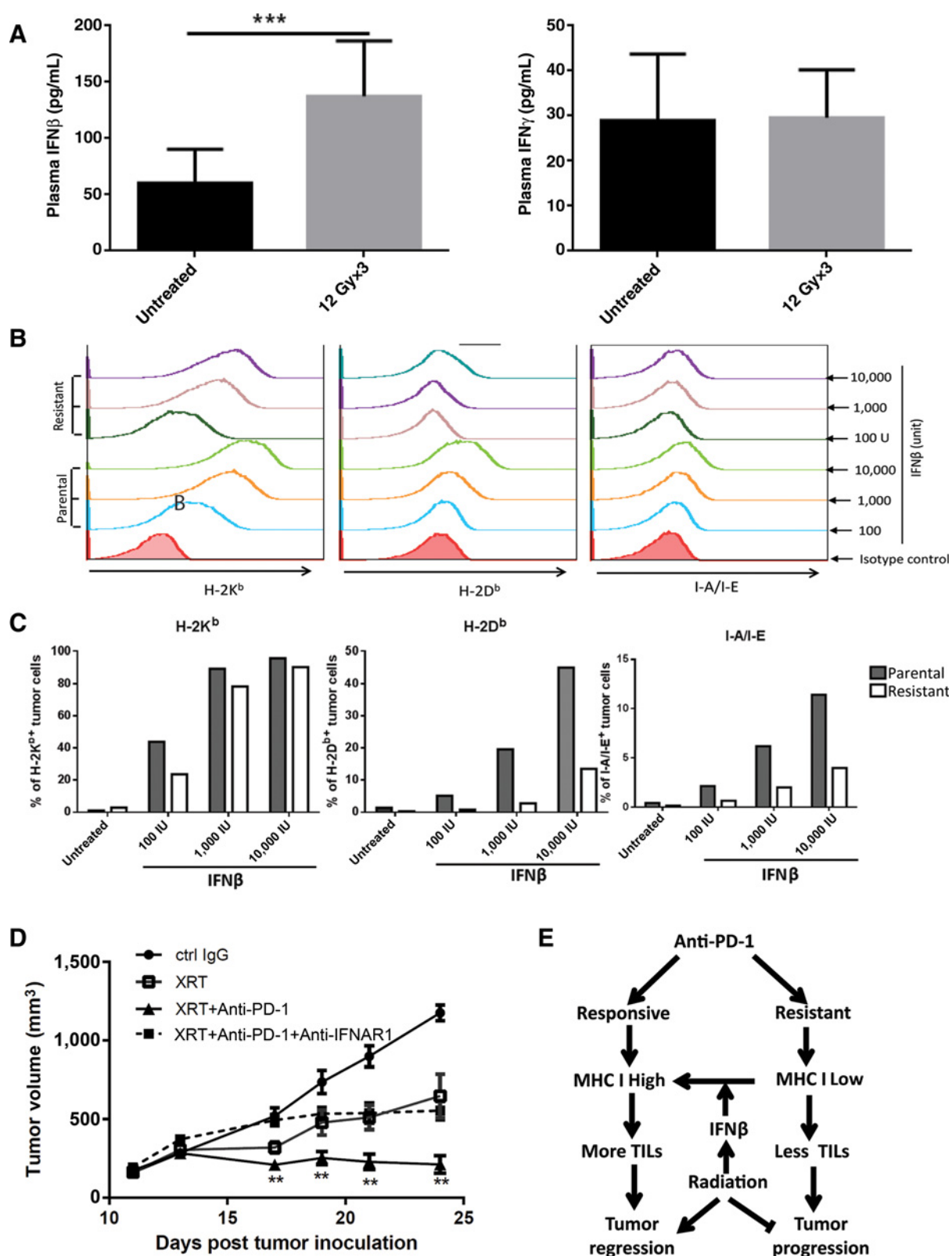


Figure 6. Radiation sensitizes tumors to anti-PD-1 via activating the IFNβ/IFNAR-MHC class I pathway. **A**, Radiation induced IFNβ, but not IFNγ, production. Mice bearing 344SQ_R tumors were either untreated or irradiated to a total dose of 36 Gy, given in three daily 12-Gy fractions. (Continued on the following page.)

(Supplementary Fig. S1A). Similarly, PD-L1 expression on tumor cells from the *in vivo* tissues were no different between the parental and anti-PD-1-resistant tumors, although both types of tumor cells showed increased PD-L1 expression upon treatment with anti-PD-1 (Supplementary Fig. S1B). Differences in anti-PD-1 antibody sensitivity in different tumor models have been attributed to differences in the extent of PD-1 blockade on T cells (13), but we found that anti-PD-1 antibody efficiently blocked PD-1 on tumor-infiltrating lymphocytes (TIL) in both parental and resistant tumors (Supplementary Fig. S1C). This suggests that the inferior response to anti-PD-1 antibody in the 344SQ_R model is not due to lack of blocking PD-L1/PD-1 signaling on TILs. Nevertheless, the similar PD-L1 expression level in 344SQ_P and 344SQ_R tumors suggests that in our model, the resistant phenotype is not due to PD-L1 expression.

Downregulation of MHC complex expression on anti-PD-1-resistant tumors

Because downregulation of MHC class I molecules is a general mechanism of tumor evasion, this pathway could be considered a top mechanistic candidate for anti-PD-1 resistance. Therefore, we measured the expression of MHC class I (H-2K^b and H-2D^b) and MHC class II (I-A/I-E) on the parental and resistant tumor cells from both *in vitro* and *in vivo* samples. The cell surface expression of H-2K^b, H-2D^b, and I-A/I-E was not detectable from the *in vitro*-cultured 344SQ_P and 344SQ_R cells (data not shown). However, coculture of 344SQ_P tumor cells (gated on CD45⁻ population) with syngeneic splenocytes (CD45⁺ population) led to significant upregulation of H-2D^b, H-2K^b, and I-A/I-E on the tumor cell surface, although I-A/I-E expression was much lower than H-2D^b and H-2K^b expression (Fig. 2A). Expression of H-2D^b, H-2K^b, and I-A/I-E remained low or absent on the surfaces of 344SQ_R tumor cells (CD45⁻ population) even after coculture with syngeneic splenocytes (CD45⁺ population; Fig. 2A). Analysis of *in vivo* tumor samples also showed that untreated resistant tumor cells had significantly lower H-2K^b than did untreated parental tumor cells (Fig. 2B). Anti-PD-1 treatment tended to increase H-2K^b expression on parental tumors, but it failed to do so on the resistant tumors. β 2-Microglobulin, a necessary component of MHC class I molecules, was downregulated in resistant tumors as well (Fig. 2C). Furthermore, tumor-infiltrating antigen-presenting cells, such as CD11b⁺Gr1⁺ cells, also expressed lower levels of H-2K^b and H-2D^b (Supplementary Fig. S2), further suggesting that downregulation of MHC class I and II expression on resistant tumors could contribute to anti-PD-1 resistance.

Reduced infiltration and function of TILs in anti-PD-1-resistant tumors

Antitumor responses are associated with the numbers and phenotypes of immune cells that infiltrate into tumors (14); having abundant TILs at diagnosis is associated with better prognosis (5, 7, 14). To understand antitumor immune profiling between the parental and resistant tumors, we isolated tumor-associated immune cells for flow cytometry analysis. Percentages of both CD4⁺ and CD8⁺ TILs were significantly reduced in the resistant tumors compared with the parental tumors (Fig. 3A and B). Anti-PD-1 treatment drastically increased the numbers of CD45⁺ immune cells, CD4⁺ and CD8⁺ T cells in the parental tumors (Fig. 3C and D), which were significantly reduced in the resistant tumors. Furthermore, the percentage of CD11b⁺Gr1⁺ myeloid cells (presumably myeloid-derived suppressor cells) within the CD45⁺ tumor-infiltrating immune cells was also increased in the resistant tumors (Supplementary Fig. S3A). The percentage of Foxp3⁺ regulatory CD4⁺ T cells (Treg) increased after anti-PD-1 treatment in both parental and resistant models (Supplementary Fig. S3B and S3C). However, no significant difference was found in Foxp3⁺ Treg percentage between parental and resistant tumors (Supplementary Fig. S3B and S3C). Furthermore, anti-PD-1 treatment drastically increased IFN γ -producing CD4⁺ and CD8⁺ TILs, two major antitumor helper or effector T cells, in parental tumors but not in resistant tumors (Fig. 3E). These findings suggest that anti-PD-1-resistant tumors have defective antitumor immune responses.

Radiation increases MHC class I expression and overcomes anti-PD-1 resistance

A majority of patients do not respond to anti-PD-1, driving us to seek strategies to overcome PD-1 resistance. Radiation is a standard of care for local tumor control. Radiation kills tumor cells by directly or indirectly damaging DNA. Radiation can also enhance antigen presentation by increasing tumor antigen release and upregulating MHC class I expression (15, 16). Thus, we hypothesized that anti-PD-1-resistant tumors could be resensitized to anti-PD-1 treatment via local radiation. We first studied whether radiation could induce MHC class I expression on 344SQ-resistant tumor cells. A relatively high-dose radiation was given (36 Gy given in three daily 12-Gy fractions), because high-dose radiation has been shown to have immunostimulatory action (17). At 6 days after treatment, tumors were isolated and stained for flow cytometry analysis of cell surface MHC class I and II expression. Radiation significantly increased H-2D^b and H-2K^b but not I-A/I-E expression on the tumor cells (Fig. 4A), which is consistent with other studies

(Continued.) Five days later, plasma was collected for cytokine detection (via Multiplex). **B** and **C**, Both histograms (**B**) and bar graphs (**C**) of mean fluorescence intensity from flow cytometry show dose-dependent induction of MHC-I (H-2K^b and H-2D^b) and MHC class II (I-A/I-E) by IFN β . For these studies, 344SQ_P and 344SQ_R cells were cultured *in vitro* and treated with IFN β (100–10,000 U/mL) for 24 hours. Cells were then stained for cell surface expression of H-2K^b, H-2D^b, and I-A/I-E and subjected to flow cytometry. Experiments were repeated twice. **D**, Radiation-induced sensitization to anti-PD-1 is blunted by antibody blockade of the IFNAR1. Mice bearing anti-PD-1-resistant 344SQ tumors were treated with radiation (36 Gy in three daily 12-Gy fractions) and anti-PD-1 (10 mg/kg, i.p. injection), with or without anti-IFNAR1 (1 mg/kg, i.t. injection). Tumor growth was monitored. *P* values were <0.05 or <0.01 for XRT + anti-PD-1 versus XRT + anti-PD-1 + anti-IFNAR1 groups from day 17 to 24 (the endpoint). Data represent means \pm SD for an *n* of 7, with experiments repeated twice. **E**, Model of anti-PD-1 resistance. Tumors that respond to treatment with anti-PD-1 express higher levels of MHC class I, which can stimulate TIL proliferation and activation, promoting strong antitumor immune responses that cause tumor regression. In contrast, anti-PD-1-resistant tumors express relatively lower levels of MHC class I and thus have less T-cell proliferation and activation. As a result, defective antitumor immunity cannot control (ctrl) tumors, and tumors continue progressing. Radiation induces type I IFN, which enhances MHC I expression, resulting in resensitization to anti-PD-1 treatment. **, *P* < 0.01; ***, *P* < 0.001.

(18). Next, we investigated whether radiation could overcome anti-PD-1 resistance *in vivo*. Anti-PD-1 treatment had no significant effect on the resistant tumors, but radiation alone significantly reduced the growth of these tumors, and the combination of radiation and anti-PD-1 treatment significantly reduced tumor growth relative to radiation or anti-PD-1 treatment alone (Fig. 4B).

Radiation plus anti-PD-1 induces tumor regression and increases proportions of CD8⁺ T cells in both irradiated and nonirradiated tumors

In the parental tumor model with tumor cells inoculated at two different sites (the secondary tumors were inoculated 10 days after the primary tumors and the anti-PD-1 treatment was started on day 14), anti-PD-1 showed good control of secondary tumors and reduced the numbers of spontaneous lung metastases but did not affect primary large tumors (Fig. 5A). For primary tumors, the combination of anti-PD-1 plus radiation not only significantly reduced primary tumor growth (Fig. 5A, top) but also significantly controlled the nonirradiated tumors and reduced spontaneous lung metastases (i.e., had abscopal effects; Fig. 5A, middle and bottom). As a result, radiation combined with anti-PD-1 resulted in complete tumor regression in 2 of 8 tumor-bearing mice. Moreover, the surviving mice rejected tumors when rechallenged with the same tumor cells (data not shown), suggesting that antitumor memory had been generated after the combination therapy. The combination treatment further increased the percentages of cytolytic effector CD8⁺ T cells but not those of CD4⁺ T cells in both irradiated and nonirradiated tumors (Fig. 5B), suggesting increased systemic antitumor immunity.

Radiation sensitizes tumors to anti-PD-1 treatment via activating the IFN β /IFNAR–MHC class I pathway

Radiation has been shown to induce type I IFN, which increases MHC class I expression and antigen presentation (15, 16). We found that IFN β but not IFN γ was increased by radiation in the anti-PD-1-resistant tumor model (Fig. 6A). Furthermore, *in vitro* treatment of 344SQ_P and 344SQ_R cells with IFN β induced dose-dependent increases in H-2K^b, H-2D^b, and I-A/I-E expression, although the induction of MHC molecules on 344SQ_R was less prominent than on 344SQ_P cells (Fig. 6B and C). Thus, we hypothesized that radiation enhanced anti-PD-1 responses via activating the IFN β /IFNAR–MHC pathway. To test this hypothesis, we tested whether blockade of type I IFN signaling would blunt the effect of radiation on overcoming anti-PD-1 resistance. We administered anti-IFNAR1 antibody along with radiation and anti-PD-1 in the anti-PD-1-resistant model and found that after IFN β signaling was blocked, radiation plus anti-PD-1 could not further reduce tumor growth relative to radiation alone (Fig. 6D), suggesting that radiation overcame anti-PD-1 responses via activating type I IFN signaling. Blocking type I IFN responses further reduced MHC class I (H-2K^b) expression on tumor cells in the radiotherapy (XRT) + anti-PD-1 + anti-IFNAR1 group compared with the XRT + anti-PD-1 group (Supplementary Fig. S4A and S4B). The number of CD4⁺ TILs, but not CD8⁺ TILs, was significantly reduced (Supplementary Fig. S4C and S4D). Finally, blocking type I IFN responses did not affect the percentage of CD4⁺Foxp3⁺ Tregs within the CD4⁺ TILs (Supplementary Fig. S4E).

Discussion

Lung cancer is the most common cause of cancer mortality globally, representing 13% of all cancer diagnoses each year and nearly 1 in 5 cancer-related deaths. For patients with early-stage disease, surgery or radiation offers a chance for cure (19), yet in the vast majority of patients, disease presents with nodal or metastatic involvement, which is rarely curable. New treatments that harness the immune system to fight lung cancer have advanced quickly to address the plight of these patients. Encouraging clinical trial results led to the approval of nivolumab (a human PD-1–blocking antibody from Bristol-Myers Squibb) by the FDA in March 2015 for the treatment of squamous NSCLC that had failed chemotherapy. Another anti-PD-1 antibody from Merck, pembrolizumab (Keytruda), was also approved for the treatment of advanced NSCLC that expresses PD-L1. Nevertheless, most patients with lung cancer do not respond to these therapies, and even among those who do, many subsequently develop disease progression. Rates of nonresponse or resistance to PD-1/PD-L1–targeted immunotherapy remain high and still represent a major challenge in current immunotherapy.

MHC class I antigen presentation to cytotoxic T lymphocytes is a crucial prerequisite for successful immune recognition and elimination of transformed cells (20). Previous studies have provided evidence that the deficiency of MHC class I complexes is a mechanism of acquired resistance to immunotherapy (21–23). A recent study further reported a truncating mutation in the gene encoding β 2M in 1 of 4 metastatic melanoma patients who were resistant to anti-PD-1 therapy (pembrolizumab; ref. 24). We found downregulation of MHC class I and II in anti-PD-1–resistant tumors in flow cytometry analysis. We also confirmed downregulation of β 2M (Fig. 2C), a necessary component of MHC class I molecules, which further contributes to MHC class I deficiency (25). Thus, blockade of the PD-L1/PD-1 pathway would not be expected to activate antitumor responses in anti-PD-1–resistant tumors, because the first signal for T-cell activation (MHC class I/antigen peptides to T-cell receptor) is lacking. Thus, the defect in the antigen presentation pathway would confer resistance to anti-PD-1 treatment, as blockade of the PD-1/PD-L1 pathway can only enhance ongoing immune responses against tumor antigens. It is known that reduction of the antigen presentation pathway leads to less T-cell activation and proliferation. Thus, when levels of MHC class I and II expression are low, fewer T cells and IFN γ -producing antitumor T cells are present in the resistant tumors. Clinical studies of anti-PD-1 nonresponding tumors have shown reduced numbers of TILs in these tumors (7), findings similar to what we observed in the anti-PD-1–resistant tumor model (Fig. 6E).

Radiation is well known to have direct cytotoxic effect to cancer cells by inducing lethal DNA damage (26), which may explain why radiation alone could reduce tumor growth in the anti-PD-1–resistant tumor model (Figs. 4B and 5A). Similarly, in an anti-CTLA-4–resistant tumor model, the resistant tumors were sensitive to radiation (27). More interestingly, combining radiation with anti-PD-1 treatment sensitized or enhanced the anti-PD-1 response in both anti-PD-1–resistant and the anti-PD-1–responding parental tumor models (Figs. 4B and 5A). Combining radiation and anti-PD-L1 also synergistically enhanced the antitumor response in a mouse melanoma model (28). The mechanism could be explained as follows: Local ablative radiation of established tumors can lead to

increased T-cell priming and T-cell-dependent tumor regression via induction of type I IFN-dependent innate and adaptive immunity (15, 16, 29). Type I IFN is a potent inducer of MHC expression. Indeed, radiation induced IFN β production in our study, which increased MHC class I expression on both parental and anti-PD-1-resistant tumor cells. Accompanied by induction of surface expression of MHC class I molecules, radiation-induced increases in the numbers or diversity of the peptide pool led to an overall increase in the number and density of surface peptide/MHC class I complexes expressed on dendritic cells (DC; ref. 18). A recent study involving whole-exome sequencing of NSCLC tumors from patients treated with pembrolizumab (anti-human PD-1) showed that higher non-synonymous mutation burden in tumors was associated with improved objective response, durable clinical benefit, and progression-free survival; efficacy also correlated with higher neoantigen burden and DNA repair pathway mutations; each of these factors was also associated with mutation burden (6). As such, the effect of radiation on generating mutations and releasing neoantigens, as well as stimulating type I IFN-MHC class I pathway, supports the contention that radiation could be an effective means of overcoming anti-PD-1/PD-L1 resistance in patients. Although we did not study the source of radiation-induced IFN β in our model, others have shown that radiation induces IFN β production by tumor-infiltrating CD11c⁺ myeloid DCs, rather than the CD45⁻ malignant compartment or other myeloid cells, in the B16F1 melanoma model (15) and in mouse models of colorectal carcinoma (28). In the latter study, the authors further showed that cyclic GMP-AMP synthase (cGAS)- and stimulator of IFN genes (STING)-dependent cytosolic DNA-sensing pathways in CD11c⁺ DCs are required for type I IFN induction after ionizing radiation (16). The induction of type I IFN also correlates with the cross-priming activity of DCs after radiation. We are now expanding on our preclinical findings with clinical trials evaluating the combination of anti-PD-1 plus radiation for stage IV NSCLC, brain metastases from NSCLC, mesothelioma, and SCLC in an effort to validate our preclinical findings regarding radiation's ability to enhance the response rate to anti-PD-1.

In conclusion, we have generated what we believe to be the first preclinical tumor model of anti-PD-1 resistance, which may be particularly relevant to patients with lung cancer that expresses PD-L1 but does not respond to anti-PD-1/PD-L1-targeted immunotherapy. Similar to human lung cancers, which have high rates of mutation in the oncogene *KRAS* and in the tumor suppressor *TP53* (30), our mouse model contains *p53* and *Kras* mutations. Furthermore, the numbers and frequency of TILs were significantly lower in the anti-PD-1-resistant tumors in this study, a finding similar to clinical observations (5). In addition, our models have downregulation of β 2M, which was reported in an anti-PD-1-

resistant patient from a recent study (24). Our preclinical findings suggest that the mechanism underlying anti-PD-1 resistance is linked to a defect in the antigen presentation pathway. Finally, we identified how radiation can be used for applications beyond local control to help prime a systemic immune response and potentially overcome anti-PD-1 resistance. If our findings are validated clinically, this could prompt a paradigm shift in the management of anti-PD-1-resistant tumors and hopefully allow the potential benefits of immunotherapy to be extended to greater numbers of patients.

Disclosure of Potential Conflicts of Interest

P. Sharma is a consultant/advisory board member for Amgen, BMS, and GSK. No potential conflicts of interest were disclosed by the other authors.

Authors' Contributions

Conception and design: X. Wang, R. Komaki, S.M. Hahn, J.W. Welsh
Development of methodology: X. Wang, D.R. Valdecanas, F. Zang, J.W. Welsh
Acquisition of data (provided animals, acquired and managed patients, provided facilities, etc.): X. Wang, J.E. Schoenhals, A. Li, D.R. Valdecanas, H. Ye, F. Zang, M. Tang, C.-G. Liu, X. Liu, S. Krishnan, M.A. Cortez, J.W. Welsh
Analysis and interpretation of data (e.g., statistical analysis, biostatistics, computational analysis): X. Wang, J.E. Schoenhals, D.R. Valdecanas, W.W. Overwijk, J.Y. Chang, J.W. Welsh
Writing, review, and/or revision of the manuscript: X. Wang, J.E. Schoenhals, C. Tang, J.P. Allison, P. Sharma, P. Hwu, R. Komaki, W.W. Overwijk, D.R. Gomez, J.Y. Chang, J.W. Welsh
Administrative, technical, or material support (i.e., reporting or organizing data, constructing databases): D.R. Gomez, S.M. Hahn
Study supervision: X. Wang, D.R. Valdecanas, J.W. Welsh

Acknowledgments

The authors thank Dr. Jonathan Kurie (MD Anderson) for his generous gift of the 344SQ parental cell line and Dr. Michael Curran for helpful discussions. We also appreciate the editorial contributions of Christine F. Wogan of MD Anderson's Division of Radiation Oncology. We also thank members of the flow cytometry and sequencing and noncoding RNA core facilities at MD Anderson for their help.

Grant Support

This work was supported by Merck & Co., Inc., Kenilworth, NJ, which provided drug and financial support for the study (LKR 142921), an MD Anderson Knowledge Gap award, Doctors Cancer Foundation Grant, The Lung Cancer Research Foundation, Cancer Center Support (Core) GrantCA016672 from the NCI (to The University of Texas MD Anderson Cancer Center), the Mabuchi Research fund, the family of M. Adnan Hamed, the Susan and Peter Goodwin Foundation, and the Orr Family Foundation (to MD Anderson Cancer Center's Thoracic Radiation Oncology program), and the Wiegand Foundation.

The costs of publication of this article were defrayed in part by the payment of page charges. This article must therefore be hereby marked *advertisement* in accordance with 18 U.S.C. Section 1734 solely to indicate this fact.

Received November 17, 2015; revised October 4, 2016; accepted October 22, 2016; published OnlineFirst November 7, 2016.

References

- Topalian SL, Drake CG, Pardoll DM. Targeting the PD-1/B7-H1(PD-L1) pathway to activate anti-tumor immunity. *Curr Opin Immunol* 2012; 24:207-12.
- Brahmer JR, Tykodi SS, Chow LQ, Hwu WJ, Topalian SL, Hwu P, et al. Safety and activity of anti-PD-L1 antibody in patients with advanced cancer. *N Engl J Med* 2012;366:2455-65.
- Topalian SL, Hodi FS, Brahmer JR, Gettinger SN, Smith DC, McDermott DF, et al. Safety, activity, and immune correlates of anti-PD-1 antibody in cancer. *N Engl J Med* 2012;366:2443-54.
- Gettinger S, Herbst RS. B7-H1/PD-1 blockade therapy in non-small cell lung cancer: current status and future direction. *Cancer J* 2014;20:281-9.
- Tumeh PC, Harview CL, Yearley JH, Shintaku IP, Taylor EJ, Robert L, et al. PD-1 blockade induces responses by inhibiting adaptive immune resistance. *Nature* 2014;515:568-71.
- Rizvi NA, Hellmann MD, Snyder A, Kvistborg P, Makarov V, Havel JJ, et al. Cancer immunology. Mutational landscape determines sensitivity to PD-1 blockade in non-small cell lung cancer. *Science* 2015; 348:124-8.

Wang et al.

7. Mella M, Kauppila JH, Karihtala P, Lehenkari P, Jukkola-Vuorinen A, Soini Y, et al. Tumor infiltrating CD8 T lymphocyte count is independent of tumor TLR9 status in treatment naive triple negative breast cancer and renal cell carcinoma. *Oncoimmunology* 2015;4:e1002726.
8. Gibbons DL, Lin W, Creighton CJ, Rizvi ZH, Gregory PA, Goodall GJ, et al. Contextual extracellular cues promote tumor cell EMT and metastasis by regulating miR-200 family expression. *Genes Dev* 2009;23:2140–51.
9. Yang Y, Ahn YH, Chen Y, Tan X, Guo L, Gibbons DL, et al. ZEB1 sensitizes lung adenocarcinoma to metastasis suppression by PI3K antagonism. *J Clin Invest* 2014;124:2696–708.
10. Sica G, Yoshizawa A, Sima CS, Azzoli CG, Downey RJ, Rusch VW, et al. A grading system of lung adenocarcinomas based on histologic pattern is predictive of disease recurrence in stage I tumors. *Am J Surg Pathol* 2010;34:1155–62.
11. Barletta JA, Yeap BY, Chirieac LR. Prognostic significance of grading in lung adenocarcinoma. *Cancer* 2010;116:659–69.
12. Swinson DE, Jones JL, Richardson D, Cox G, Edwards JG, O'Byrne KJ. Tumour necrosis is an independent prognostic marker in non-small cell lung cancer: correlation with biological variables. *Lung Cancer* 2002;37:235–40.
13. Ngiew SF, Young A, Jacquolot N, Yamazaki T, Enot D, Zitvogel L, et al. A threshold level of intratumor CD8+ T-cell PD1 expression dictates therapeutic response to anti-PD1. *Cancer Res* 2015;75:3800–11.
14. Mihm MC Jr, Mule JJ. Reflections on the histopathology of tumor-infiltrating lymphocytes in melanoma and the host immune response. *Cancer Immunol Res* 2015;3:827–35.
15. Burnette BC, Liang H, Lee Y, Chlewicki L, Khodarev NN, Weichselbaum RR, et al. The efficacy of radiotherapy relies upon induction of type I interferon-dependent innate and adaptive immunity. *Cancer Res* 2011;71:2488–96.
16. Deng L, Liang H, Xu M, Yang X, Burnette B, Arina A, et al. STING-dependent cytosolic DNA sensing promotes radiation-induced type I interferon-dependent antitumor immunity in immunogenic tumors. *Immunity* 2014;41:843–52.
17. Lee Y, Auh SL, Wang Y, Burnette B, Wang Y, Meng Y, et al. Therapeutic effects of ablative radiation on local tumor require CD8+ T cells: changing strategies for cancer treatment. *Blood* 2009;114:589–95.
18. Reits EA, Hodge JW, Herberts CA, Groothuis TA, Chakraborty M, Wansley EK, et al. Radiation modulates the peptide repertoire, enhances MHC class I expression, and induces successful antitumor immunotherapy. *J Exp Med* 2006;203:1259–71.
19. Chang JY, Senan S, Paul MA, Mehran RJ, Louie AV, Balter P, et al. Stereotactic ablative radiotherapy versus lobectomy for operable stage I non-small-cell lung cancer: a pooled analysis of two randomised trials. *Lancet Oncol* 2015;16:630–7.
20. Aptsiauri N, Cabrera T, Garcia-Lora A, Lopez-Nevot MA, Ruiz-Cabello F, Garrido F. MHC class I antigens and immune surveillance in transformed cells. *Int Rev Cytol* 2007;256:139–89.
21. Restifo NP, Marincola FM, Kawakami Y, Taubenberger J, Yannelli JR, Rosenberg SA. Loss of functional beta 2-microglobulin in metastatic melanomas from five patients receiving immunotherapy. *J Natl Cancer Inst* 1996;88:100–8.
22. D'Urso CM, Wang ZG, Cao Y, Tataka R, Zeff RA, Ferrone S. Lack of HLA class I antigen expression by cultured melanoma cells FO-1 due to a defect in B2m gene expression. *J Clin Invest* 1991;87:284–92.
23. Sucker A, Zhao F, Real B, Heeke C, Bielefeld N, Mabetan S, et al. Genetic evolution of T-cell resistance in the course of melanoma progression. *Clin Cancer Res* 2014;20:6593–604.
24. Zaretsky JM, Garcia-Diaz A, Shin DS, Escuin-Ordinas H, Hugo W, Hu-Lieskova S, et al. Mutations associated with acquired resistance to PD-1 blockade in melanoma. *N Engl J Med* 2016;375:819–29.
25. Ardeniz O, Unger S, Onay H, Ammann S, Keck C, Cianga C, et al. β 2-Microglobulin deficiency causes a complex immunodeficiency of the innate and adaptive immune system. *J Allergy Clin Immunol* 2015;136:392–401.
26. Ross GM. Induction of cell death by radiotherapy. *Endocr Relat Cancer* 1999;6:41–4.
27. Twyman-Saint Victor C, Rech AJ, Maitly A, Rengan R, Pauken KE, Stelekati E, et al. Radiation and dual checkpoint blockade activate non-redundant immune mechanisms in cancer. *Nature* 2015;520:373–7.
28. Deng L, Liang H, Burnette B, Beckett M, Darga T, Weichselbaum RR, et al. Irradiation and anti-PD-L1 treatment synergistically promote antitumor immunity in mice. *J Clin Invest* 2014;124:687–95.
29. Lim JY, Gerber SA, Murphy SP, Lord EM. Type I interferons induced by radiation therapy mediate recruitment and effector function of CD8(+) T cells. *Cancer Immunol Immunother* 2014;63:259–71.
30. Ding L, Getz G, Wheeler DA, Mardis ER, McLellan MD, Cibulskis K, et al. Somatic mutations affect key pathways in lung adenocarcinoma. *Nature* 2008;455:1069–75.

Cancer Research

The Journal of Cancer Research (1916–1930) | The American Journal of Cancer (1931–1940)

Suppression of Type I IFN Signaling in Tumors Mediates Resistance to Anti-PD-1 Treatment That Can Be Overcome by Radiotherapy

Xiaohong Wang, Jonathan E. Schoenhals, Ailin Li, et al.

Cancer Res 2017;77:839-850. Published OnlineFirst November 7, 2016.

Updated version Access the most recent version of this article at:
doi:[10.1158/0008-5472.CAN-15-3142](https://doi.org/10.1158/0008-5472.CAN-15-3142)

Supplementary Material Access the most recent supplemental material at:
<http://cancerres.aacrjournals.org/content/suppl/2016/11/05/0008-5472.CAN-15-3142.DC1>

Cited articles This article cites 30 articles, 10 of which you can access for free at:
<http://cancerres.aacrjournals.org/content/77/4/839.full.html#ref-list-1>

E-mail alerts [Sign up to receive free email-alerts](#) related to this article or journal.

Reprints and Subscriptions To order reprints of this article or to subscribe to the journal, contact the AACR Publications Department at pubs@aacr.org.

Permissions To request permission to re-use all or part of this article, contact the AACR Publications Department at permissions@aacr.org.